JACS
JOURNAL OF THE AMERICAN CHEMICAL SOCIETY
Article
pubs.acs.org/JACS

Hydrophobic Forces, Electrostatic Steering, and Acid–Base Bridging between Atomically Smooth Self-Assembled Monolayers and End-Functionalized PEGolated Lipid Bilayers

Markus Valtiner,[†] Stephen H. Donaldson, Jr.,[†] Matthew A. Gebbie,[‡] and Jacob N. Israelachvili*[,†,‡]

[†]Department of Chemical Engineering, University of California Santa Barbara (UCSB), Santa Barbara, California 93106-5080, United States

[‡]Materials Department, University of California Santa Barbara (UCSB), Santa Barbara, California 93106, United States

Supporting Information

ABSTRACT: A molecular level understanding of interaction forces and dynamics between *asymmetric* apposing surfaces (including end-functionalized polymers) in water plays a key role in the utilization of molecular structures for smart and functional surfaces in biological, medical, and materials applications. To quantify interaction forces and binding dynamics between asymmetric apposing surfaces in terms of their chemical structure and molecular design we developed a novel surface forces apparatus experiment, using self-assembled monolayers (SAMs) on *atomically smooth* gold substrates. Varying the SAM head group functionality allowed us to quantitatively identify, rationalize, and therefore control which interaction forces dominated between the SAM surfaces and a surface coated with short-chain, amine end-functionalized polyethylene glycol (PEG) polymers extending from a lipid bilayer. Three different SAM-terminations were chosen for this study: (a) carboxylic acid, (b) alcohol, and (c) methyl head group terminations. These three functionalities allowed for the quantification of (a) specific acid–base bindings, (b) steric effects of PEG chains, and (c) adhesion of hydrophobic segments of the polymer backbone, all as a function of the solution pH. The pH-dependent acid–base binding appears to be a *specific and charge mediated hydrogen bonding interaction* between oppositely charged carboxylic acid and amine functionalities, at pH values above the acid pK_A and below the amine pK_A. The long-range electrostatic "steering" of acid and base pairs leads to remarkably rapid binding formation and high binding probability of this specific binding even at distances close to full extension of the PEG tethers, a result which has potentially important implications for protein folding processes and enzymatic catalysis.

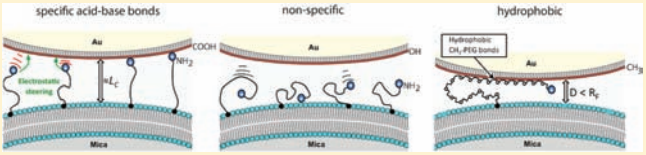

INTRODUCTION

Biological and synthetic end-functionalized, short-chain polymers that are terminally bound to surfaces are centrally important in biology, medical, and materials applications because they can mediate cell interactions, impact the stability of colloidal solutions, and provide targeted functionality at an interfaces.[1−4] An understanding, and ultimately control of interfaces that expose end-functionalized polymer tethers will aid in the development of tunable architectures for biomaterial interfaces in implants, bioinspired surface coatings, and functional vesicles for drug delivery applications.[5] Unlike colloidal interactions in bulk solution, which occur mainly between similar or "symmetric" particles, many biological and synthetic systems are comprised of dissimilar interacting surfaces, such as biomembrane tissue interactions,[6] biofilm or cell–surface interactions,[7] surface–adhesive or surface–coating interactions,[3,4] and sensor–analyte interactions.[8]

In particular, *specific asymmetric interactions* such as acid–base binding or biosensitive (*e.g.*, ligand–receptor or lock-and-key) binding, as well as their effective range and molecular dynamics, not only play a central role in biological processes such as protein folding[9] or enzymatic catalysis[10,11] but also can trigger structure and functionality in synthetic systems such as supramolecular assemblies,[12] mesoscale materials,[13] and metal organic frameworks.[14] For instance, rationalizing protein folding in terms of a directed steering of macromolecular interactions due to long-range hydrophobic and electrostatic forces[15,16] resolves what has become famous as Levinthal's paradox,[17] which states that proteins fold reliably and rapidly into their unique native state, despite the vast number of possible configurations and degrees of freedom. In materials science, long-range forces in triblock copolymers were successfully utilized to trigger specific mesoporous silica or zeolite structures.[13,18] Understanding and quantifying the interplay and dynamics of these specific interactions, and persistent nonspecific interactions such as van der Waals, hydrophobic, steric forces, Coulombic, and electric double layer forces, is essential for providing a framework for the design of composite materials at the nanoscale and mesoscale,[19−21] understanding biological processes, controlling adhesion in various systems, and optimizing and utilizing interactions of materials with their environment.[2]

Received: October 13, 2011
Published: December 16, 2011

 © 2011 American Chemical Society dx.doi.org/10.1021/ja209653n | *J. Am. Chem.Soc.* 2012, 134, 1746–1753

Currently, the lack of full understanding of the interaction forces at polymer-functionalized interfaces in terms of their chemical and molecular structure contributes to the difficulty in designing tunable and responsive materials and surfaces with long-range structuring and long-term predictable properties. This work aims to improve the understanding of the different interactive forces arising from the different chemical functionalities on surfaces and complementary apposing polymer-modified interfaces.

For many years, self-assembled alkanethiol monolayers (SAMs) on gold have been successfully used for the targeted design of surface properties such as wettability, hydrophobicity, and adhesivity, with techniques such as molecular imprinting allowing the design and fabrication of arbitrary two-dimensional organic patterns.[22,23] The ability to make atomically smooth gold surfaces with Å-level roughness[24] allowed for the design and use of surfaces coated with molecularly smooth self-assembled monolayers for surface forces apparatus (SFA) experiments. As the apposing surface we used a lipid-bilayer that exposed end-functionalized polyethylene glycol (PEG) molecules (PEGolated lipid bilayers) into the water phase. PEGolation of lipid bilayers has been successfully used to measure receptor−ligand bindings with the SFA;[25,26] PEG acts as steric stabilizer for liposomes and colloidal solutions[1] and end-functionalized PEG chains provide interesting possibilities for targeted design of solid−liquid interfaces.

In the newly developed asymmetric systems studied here, the PEG polymer chains on the bilayer surface were end-functionalized with an amine head group facing an atomically smooth gold surface modified by antipodal SAM-chemistries. Figure 1 shows the molecules used for the surface

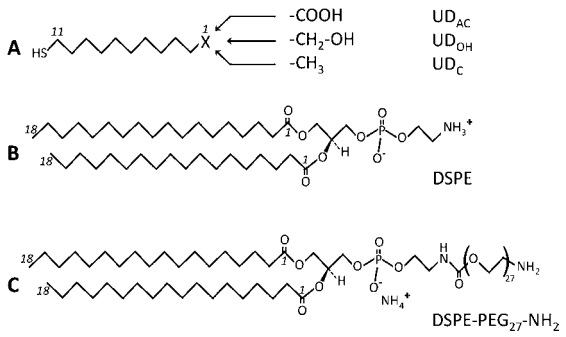

Figure 1. Alkanethiols used for SAM formation on gold and lipid amphiphiles used for bilayer formation on mica: (A) 11-Thiol-undecanecarboxylic-acid (UD_{AC}), 11-Thiol-undecane-1-ol (UD_{OH}), and 1-Undecanethiol (UD_C). (B) 1,2-Distearoyl-*sn*-glycero-3-phosphoethanolamine (DSPE). (C) 1,2-Distearoyl-*sn*-glycero-3-phosphoethanolamine-*N*-[amino(polyethylene glycol)-2000] ammonium salt ($DSPE\text{-}PEG_{27}\text{-}NH_2$).

modifications. The SAMs used in this study had (a) carboxylic acid, (b) alcohol, and (c) methyl head group terminations. PEG-molecules were incorporated into the bilayer at a low surface coverage (σ = 0.7%) in order to minimize the lateral interactions of neighboring PEG chains, providing a surface covered by end-functionalized PEG "mushrooms" in a good solvent.

Figure 2 shows a schematic of the designed SFA experiment. Using this experimental setup we show how SAM modifications and PEGolated lipid bilayer chemistry impact the interactive forces between apposing surfaces by varying the apposing SAM head group functionality and the solution pH. We discuss how our results shed new light into the interaction of asymmetric systems and dissimilar surfaces, especially how different functionalities at the molecular level change the adhesive binding mechanism and modify long-range steering interactions, which shape structure−property relationships of materials.

EXPERIMENTAL DESIGN

Interaction Force Measurements with the Surface Forces Apparatus. We use the surface forces apparatus (SFA) to measure both attractive and repulsive interaction forces between two apposing surfaces. All force measurements were performed using an SFA-2000 setup, which has been previously described.[27] In these experiments, we measure dynamic force−distance (F/D) curves between two cylindrical surfaces (with a radius of curvature R = 2 cm) in crossed cylinder geometry during the approach and separation of the two apposing surfaces. Measurements were done at 22 °C, and only normal forces are reported in this study. F/D profiles were very reproducible over multiple experimental runs, for both different contact positions and different setups. Representative profiles are presented. The separation distance, forces, and surface geometry were simultaneously measured by visualization of so-called fringes of equal chromatic order (FECO) using white light interferometry. For this work, forces were measured with an accuracy of about 10 nN/m and distances were measured with an accuracy of ±2.5 Å. For details the reader is referred to our earlier work.[27,28]

Surface Preparations. Atomically smooth gold surfaces were prepared using templating techniques.[24,29,30] First, a freshly cleaved mica sheet with a thickness from 15 to 25 μm was coated with a 42.5 nm thick gold layer. Next, the mica sheet was glued gold-down onto a cylindrical glass disk (with a radius of R = 2 cm) using a UV-curable glue (Norland Adhesives, NOA81). Prior to curing, the glue was degassed under vacuum for at least 30 min to avoid the formation of gas bubbles underneath the gold surface. After fully curing the glue, the mica-sheet was stripped off in ethanol (which minimizes the mechanical stress while peeling off the mica) to reveal the gold surface. The resulting gold surfaces are atomically smooth and perfectly suited for SFA measurements with well-defined surface geometries.[29,31] After stripping off the mica-sheet, freshly exposed gold surfaces were immediately placed into 1 mM ethanolic solutions of the respective alkane thiols. Figure 1**A** shows the chemical structure of the alkane thiols used in this study. After 12−24 h, the surface was taken out of the solution, washed extensively with ethanol, and then sonicated in ethanol for 30 s. Excessive sonication was avoided so that the thin gold surfaces were not damaged. Bilayers were deposited on mica using the Langmuir−Blodgett (LB) technique. The lipid molecules used in this study are illustrated in Figure 1B/C.

The first monolayer of the supported bilayers was a closely packed DSPE monolayer, which was transferred onto the mica at a surface pressure of 40 mN/m^2 and an area of 42 Å^2 per molecule. During transfer, the mica was raised through the air−water interface with a rate of 1 mm/min. DSPE monolayers are known to form strong physical bonds with the mica support through Coulombic interactions[1] and provided a smooth hydrophobic surface for the deposition of the outer layer. For the outer layer, DSPE and $DSPE\text{-}PEG_{27}\text{-}NH_2$ were spread on the surface of the trough at the desired molar ratio ($DSPE\text{-}PEG_{27}\text{-}NH_2$ density, $\sigma = (2.5 \pm 0.2) \times 10^{16}$ m^{-2}), equilibrated for at least 30 min, and then the deposition proceeded as described above. The resulting PEGolated bilayer-coated mica surface was kept under water for the remainder of an experiment because dehydration leads to destruction of the outer monolayer.[1]

Materials. All chemicals were of the highest available grade and were used without further purification. 1,2-Distearoyl-*sn*-glycero-3-phosphoethanolamine (DSPE) and 1,2-distearoyl-*sn*-glycero-3-phosphoethanolamine-*N*-[amino(polyethylene glycol)$_{27}$] ammonium salt ($DSPE\text{-}PEG_{27}\text{-}NH_2$) were obtained from Avanti Lipids. The contour length, L_C = 10.2 nm, of $DSPE\text{-}PEG_{27}\text{-}NH_2$ was calculated using a segment length of 3.65 Å for the 28 individual segments (27 PEG

dx.doi.org/10.1021/ja209653n | J. Am. Chem.Soc. 2012, 134, 1746−1753

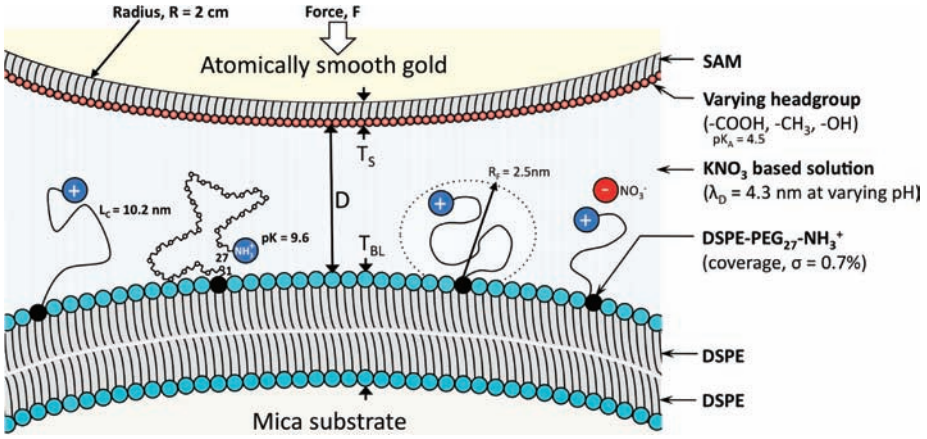

Figure 2. Schematic of the experiment and surface modifications. With a surface forces apparatus (SFA) we measured force−distance curves (F/D curves) between two dissimilar apposing cylindrical surfaces of similar radii, R = 2 cm, in crossed-cylinder geometry. All measurements were performed in KNO_3 based solutions (prepared from 5 mM HNO_3 and 5 mM KOH) of varying pH and constant Debye length λ_D = 4.3 nm using the procedures outlined in the Experimental Design section. One of the surfaces consisted of an atomically smooth gold surface that was modified by a self-assembled monolayer (SAM) of thickness, T_S. The SAMs were terminated with a carboxylic acid (pK = 4.5), an alcohol, or a methyl group as the terminal head group. For the apposing surface, mica that was coated with a DSPE lipid bilayer of thickness, T_{BL}, was used. The outer monolayer consisted of a binary mixture of DSPE and 0.7%$_{mol}$ PEGolated and amine (pK_A = 9.6) end-functionalized DSPE-PEG_{27}-NH_2 lipid. The PEG_{27}-NH_2 polymer coil has a theoretical Flory radius of R_F = 2.5 nm and a theoretical contour length of L_C = 10.2 nm (3.65 Å per segment). In an aqueous solution the terminal amine group of the PEGolated lipid is protonated and thus positively charged at pH levels <9.6. The distance D between the apposing surfaces was defined with respect to the contact of the SAM with the outer DPSE monolayer, where D = 0.

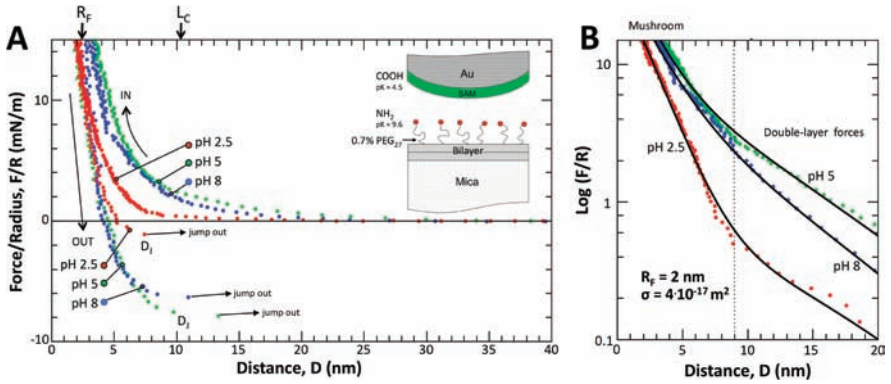

Figure 3. Forces between an end-grafted and end-functionalized PEG_{27}-NH_2 surface and a carboxylic acid terminated SAM surface in KNO_3 based aqueous solutions with an ionic strength of 5 mM at three different pH values. (A) Representative force−distance profiles measured during approach (IN) and separation (OUT). The data in (B) show the semilog plot of the same approach curves shown in (A). Different pH values are indicated. The approach curves are always repulsive and show two linear regimes with a characteristic kink at about 3−4 R_F (indicated by the dashed line) in the semilog plot in (B). At a larger separation D > 9 nm double-layer forces between the two surfaces dominate the repulsions, because in these dilute solutions the Debye length is longer then the characteristic decay length (R_F) of the steric forces. Both the steric and the double layer forces can be fit with equations for interacting mushrooms and the Hogg−Healy−Fuerstenau equation for dissimilar double layers. The solid lines in (B) correspond to the theoretical fits (normalized by the radius of curvature, R) using eq 1. The separation curves in (A) show adhesion at all measured pH levels. At pH 2.5 where the carboxylic acid is protonated and uncharged the surfaces separate and jump out at about D_j = 2−3 R_F and the lowest adhesion was measured. At pH 5 and pH 8, above the pK_A of the carboxylic acid, considerably higher adhesion forces were measured and the surfaces separate and jump out at larger distances at around L_C. The untypical U-shape of the separation curves indicate a bridging of the surfaces and specific binding of the amine at the carboxylic acid terminated SAM surface (cf. text for details).

segments plus the linker segment). For bilayer deposition DSPE was dissolved in chloroform, and DSPE-PEG_{27}-NH_2 was dissolved in a mixture of chloroform and methanol (9:1 volume fractions) prior to spreading on the LB trough. All water used in preparing experimental and LB trough solutions was particle-free and filtered through a Milli-Q (Elix 10) system. Solutions were prepared from 5 mM KOH and 5 mM HNO_3 stock solutions, which were mixed to adjust the experimental solution pH. This allowed for changing the solution pH while leaving the experimental Debye length, λ_D, constant at λ_D = 4.3 nm. Accordingly, the ratio $[H^+]/[K^+]$ decreases and the ratio of $[OH^-]/[NO_3^-]$ increases with increasing pH, and at pH 7 $[H^+] = [OH^-] = 10^{-7}$ mol/L and $[K^+] = [NO_3^-]$ = 5 mmol/L.

RESULTS AND ANALYSIS

Using the experimental system illustrated in Figure 2, measurements of the interactive forces between amine end-functionalized PEGolated lipid bilayers and molecularly smooth SAM-covered gold surfaces with three different head groups were performed. During each experiment, the pH of the aqueous solution was varied in situ from pH = 2.5 to pH = 8 at a fixed ionic strength of I = 5 mM. For these measurements, SAMs with distinctly different properties were used: a carboxylic acid terminated SAM (UD_{Ac}-SAM) that offers pH sensitive acidic groups (pK = 4.5) for the specific binding of the

dx.doi.org/10.1021/ja209653n | J. Am. Chem.Soc. 2012, 134, 1746−1753

amine end-functionalized PEG_{27}-NH_2 coil, an alcohol terminated SAM (UD_{OH}-SAM), and a hydrophobic methyl terminated SAM (UD_C-SAM). The SAMs were prepared on atomically smooth gold surfaces,[24,29,30] and the PEGolated bilayers were deposited on atomically smooth mica substrates. More details on the preparation of the surfaces are outlined in the Experimental Design section.

The SAM termination directly affects the surface energy, surface chemistry, specific binding sites, and wettability of the surfaces. Figure 3A shows the measured forces between the 0.7% PEG_{27}-NH_2 bilayer surface and the carboxylic acid terminated UD_{Ac}-SAM at varying pH levels. The approach curves (IN) reveal repulsive forces at all pH levels with two different linear regimes, as shown in the semilog plot in Figure 3B. As expected, the long-range interactions between these dissimilar surfaces are due to electric double layer forces, which dominate the force–distance characteristics from 40 nm $\geq D \geq$ 9 nm. The double layer forces increase with increasing the pH value from pH = 2.5 to pH = 5 and slightly decrease again at pH = 8. These interactions can be fit well with the experimental Debye length using the Hogg–Healy–Fuerstenau equation[32] for overlapping double layers of dissimilar surfaces using constant potential boundary conditions. The short-range repulsive interaction at distances $D \leq 9$ nm corresponds to steric forces due to the unfavorable entropy associated with compressing (and thus confining) the PEG_{27}-NH_2 polymer chains between the surfaces. These steric forces show an exponential decay with a characteristic decay length of 2 nm, which is close to the theoretical Flory radius R_F of the polymer chains (R_F = 2.5 nm). The electric double layer and the steric forces appear to be additive[33] and can be fit using a linear superposition of the van der Waals force $F_{VDW}(D)$, the electric double layer force between dissimilar surfaces,[32] $F_{EDL}(D)$, and the repulsive steric forces resulting from the confinement of the end-grafted polymer chains,[34] $F_{Mush}(D)$, given by eq 1:

$$\frac{F(D)}{2\pi R}_{[\mathrm{N/m}]} = -\frac{A_H}{6D^2} + \frac{\varepsilon\varepsilon_0}{\lambda_D}[2\varphi_A\varphi_B e^{-D/\lambda_D} - (\varphi_A^2 + \varphi_B^2)e^{-2D/\lambda_D}] + \frac{36k_BT}{\sigma}e^{-D/R_F} \quad (1)$$

with the Boltzmann constant k_B, the surface potentials ϕ_A and ϕ_B of the respective apposing surfaces, the Hamaker constant A_H, the temperature T, the dielectric permittivity in vacuum ε_0, the relative dielectric permittivity ε of the liquid medium, and the experimental Debye length, λ_D.

The separation curves in Figure 3A show a strong dependence on the pH level of the aqueous medium. The measured adhesion increases almost an order of magnitude with increasing the pH from pH 2.5 to pH 5 and decreases again slightly at pH 8. The jump out distance D_J (the point where the surfaces completely separate) also changes with the solution pH. At pH 2.5 the surfaces separate at a distance D_J of about $2-3R_F$. Therefore, the binding between the positively charged amine and the neutral carboxylic acid at pH 2.5 appears to be a relatively weak, nonspecific interaction. However, at higher pH levels of 5.5 and pH 8 the surfaces separate at much larger distances $D_J \approx L_C$. Thus, the end-functionalized PEG_{27}-NH_2 chain appears to specifically attach to the UD_{Ac}-SAM, in particular the deprotonated carboxylic acid, and the bridging of strongly bound PEG chains leads to an increased jump out distance on separation.

The fact that the surfaces separate and jump out at approximately the PEG contour length L_C is particularly interesting as this observation suggests that the PEG chains fully extend before the bridging interaction is broken. This result indicates that the head group of the PEG_{27}-NH_2 has a high affinity for the terminal SAM carboxylic acid functionalities, and this acid–base bridging interaction increases in magnitude as the pH is raised. Importantly, while the solution conditions do not facilitate an actual acid–base condensation, specific binding between the positively charged amine group ($-NH_4^+$) and the negatively charged carboxylic acid (COO^-) is clearly present at pH $\geq$ 4.5, above the pK_A of the carboxylic acid. The measured adhesive force indicates bond energies in the range of $9.5-11k_BT$ per bond,[35] which is a strong specific hydrogen bond (typical hydrogen bonds[33] range from 4 to $12k_BT$) but lower compared to, e.g., typical specific receptor–ligand bonds ($15-35k_BT$).[36]

While the specificity of an acid–base bond strongly depends on the pH level and the involved molecular pair, this binding is still a statistical process involving dynamic effects governed by the diffusivity of the polymer chain (PEG) to which the functional amine group is tethered. Statistically, an available amine group is about $0.7R_F$ away from the surface, but the probability of a successful binding at a larger distance increases with time and depends on the dynamics of the PEG chain (*cf.* Bell theory in ref 33). Figure 4 shows forces measured between a bilayer surface with 0.7% end-grafted PEG_{27}-NH_2 and a carboxylic acid terminated apposing UD_{Ac}-SAM surface at pH 8, while varying the compression magnitude and thus the minimum approach distance between the surfaces. As discussed above, these conditions enable the specific binding between the end-functionalized PEG_{27}-NH_2 chains and carboxylic acid terminated apposing surface. The approach curves (IN) have the same characteristics discussed previously and are purely repulsive. Notably, if the surfaces are separated before they approach to distances of $D \leq L_C$ then no adhesion is measured, but when the final separation distance is below the maximum

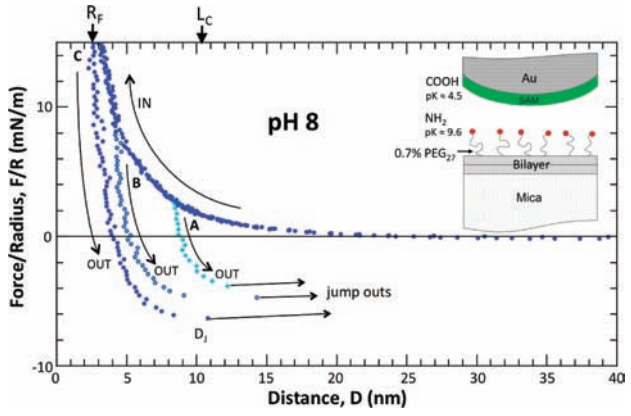

Figure 4. Forces at different compressions (A, B, and C) between an end-grafted and end-functionalized PEG_{27}-NH_2 surface and a carboxylic acid terminated SAM surface in KNO_3 based aqueous solutions with an ionic strength of 5 mM at pH = 8. At these conditions the end-functionalized polymers can bridge the two surfaces. Surfaces are approached to different final distances and compressions (IN) marked as A, B, and C and are then immediately withdrawn (OUT) (cf. text for details).

dx.doi.org/10.1021/ja209653n | J. Am. Chem.Soc. 2012, 134, 1746–1753

capture distance (i.e., the length of the fully extended polymer) $D \leq L_C$, a significant adhesion is measured on separation.

Even at low compression forces (curve A in Figure 4) of F/R = 2 mN/m and a resulting separation distance of D = 9 nm, which is about $0.9L_C$ and about 4 times R_F, an adhesive force is measured with a magnitude of 2/3 of the maximum adhesion measured at these conditions. At higher compression forces of F/R = 8 mN/m and F/R = 16 mN/m (curves B and C in Figure 4), the adhesion force F_{ad} is higher and saturated at about F/R = 6 mN/m. A significant adhesion, and thus capturing of the apposing surface, manifests at critical capture distances, D_C (at $D > D_C$ the binding probability rapidly falls to zero within a few Å),[36] considerably further from the surface than the equilibrium distance R_F of the polymer chains. Therefore, even approach distances around $0.9L_C$ (curve A in Figure 4) are sufficient to lead to significant adhesive forces. Remarkably, this observation suggests a rapid acid−base binding formation even at distances close to full extension of the PEG tethers, although the bond energy of an acid−base pair is only around $9.5-11k_BT$. Previous work on ligand−receptor bindings has shown that rapid binding formation for interaction energies in this range is expected at approximately 20% smaller critical capture distances of $D_C \leq 0.75L_C$.[25,36]

However, such models only account for the diffusive statistical motion of the polymer coils. In the present case, a nonspecific long-range electrostatic force biases the statistical motion of the PEG_{27}-NH_2 chains (and thus also the chemical equilibrium of binding/unbinding events), whereas specific noncharged receptor−ligand systems reach their final binding state by statistical motion.[25,26,36] The interplay between Brownian molecular dynamics and the attractive Coulombic interaction between acid−base pairs leads to *electrostatic steering* of the polymer head group toward the SAM surface and results in rapid formation of the final binding state with critical binding distances at larger separations compared to nonbiased systems.[36] This has potentially important implications for biocatalysis involving proton donors or acceptors.[37]

Changing the terminating head group of the apposing SAM surface from a carboxylic acid to an alcohol head group has a dramatic effect on the interactions between the surfaces. Figure 5A shows force−distance profiles measured between the 0.7% PEG_{27}-NH_2 bilayer surface and the alcohol terminated UD_{OH}-SAM at varying pH levels. At acidic conditions of pH = 2.5 both the approach (IN) and the separation profiles (OUT) reveal repulsive forces at all distances, and again the first repulsive regime is due to electrostatic double layer forces. In this case, the low surface potentials of both surfaces (0 mV for the SAM surface and about 20 mV for the PEG_{27}-NH_2 surface) leads to a greatly reduced repulsion as compared to the carboxylic acid SAM. The second linear regime at distances $D \leq 9$ nm again corresponds to steric forces that can be well described by the mushroom theory discussed above. The OH-terminated SAM does not provide specific binding possibilities, and thus steric repulsions dominate over the weak short-range van der Waals forces; consequently no adhesive force is measured on separation. At pH = 8 we find that the approach profiles are also purely repulsive with similar characteristics, but the separation profile shows a very weak adhesive force around F/R = 0.5 mN/m. This small adhesion is likely caused by increased hydrogen bonding between the PEG_{27}-NH_2 chain segments and the OH-terminated SAM surface.

Figure 5B shows the forces measured between the 0.7% PEG_{27}-NH_2 bilayer surface and the methyl terminated

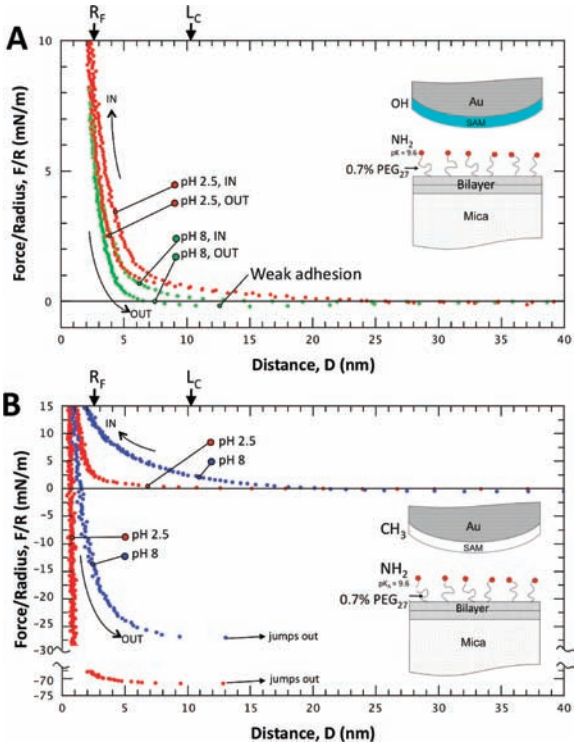

Figure 5. (A) Representative force−distance profiles between an end-grafted and end-functionalized PEG_{27}-NH_2 surface and an alcohol (OH) terminated SAM surface in KNO_3 based aqueous solutions with an ionic strength of 5 mM at pH 2.5 and pH 8 measured during approach (IN) and separation (OUT). At pH = 2.5 both approach and separation are purely repulsive because of the steric repulsions of the end-grafted PEG coils and hydration forces. At pH = 8 the approach is repulsive but the separation shows a weak adhesion (cf. text for details). (B) Representative force−distance profiles between an end-grafted and end-functionalized PEG_{27}-NH_2 surface and a methyl ($-CH_3$) terminated hydrophobic SAM surface in KNO_3 based aqueous solutions with an ionic strength of 5 mM at pH 2.5 and pH 8 measured during approach (IN) and separation (OUT) (cf. text for details).

hydrophobic UD_C-SAM at varying pH levels. The hydrophobic character of the apposing SAM surface causes remarkable differences in the measured interactions. The approach curves (IN) are purely repulsive at both pH levels, whereas the repulsive force increases significantly at the higher pH = 8 (as compared to pH = 2.5). The magnitude of the pull-off forces decreased significantly with increasing the pH from pH = 2.5 to pH = 8: from F/R = 71 mN/m at pH 2.5 to 30 mN/m at pH 8. The separation curves (OUT) reveal that the surfaces jump-out (or pull-off) at distances of $D_J \approx L_C$. Thus, it appears that the hydrophobic SAM provides the possibility for a strong hydrophobic interaction between the PEG-backbone (each segment consists of a hydrophobic $-CH_2-CH_2-$alkane segment, which is connected by a (hydrophilic) oxygen atom). The backbone can peel off the apposing surface segment by segment, until the last segment detaches at distances close to full extension of the polymer chain, giving rise to the U-shape of the separation profile. As expected, the dramatically increased adhesion also affects the contact mechanics of the surfaces. As soon as the two surfaces approach to distances around R_F a pronounced flattening of the contact was observed in the contact FECO, and at pH = 2.5 a

dx.doi.org/10.1021/ja209653n | J. Am. Chem.Soc. 2012, 134, 1746−1753

deformation of the contact was observed even after separation. The contact FECO are shown in the Supporting Information.

The force−distance profiles in Figure 5B further show that the surfaces approach to a distance $D < R_F$ indicating a considerable attraction that dominates over the steric repulsion resulting from chain confinement. The hydrophobic SAM facilitates the formation of strong hydrophobic "bonds" between the PEG backbone and the apposing surface. Since the pioneering work of Kauzman[38] it is well-known that the hydrophobic interaction and force are considerably stronger compared to van der Waals forces. The physical origin is thought to be due to water density fluctuations,[39] but there is currently no agreed-upon potential force law which describes hydrophobic interactions.[40] It is however remarkable that the measured force is strongly pH sensitive, which agrees well with previous measurements[15,41] suggesting that the increased proton concentration (or the decreased hydroxide concentration) contributes to and possibly facilitates the observed effects. Results of vibrational sum frequency generation (SFG) spectroscopy[42,43] revealed that the structure of water at an acidic hydrophobic interface is distinctly different compared to an alkaline hydrophobic interface, and water molecules can even flip their orientation under varying pH conditions. It has been argued that the adsorption of hydroxide ions to the hydrophobic interface at higher pH levels leads to an increased negative electrostatic charge and to a change of the water structure.[42] In Figure 5B, the repulsive approach curves recorded at pH 8 indicate a considerably increased electrostatic repulsion, which decays with the experimental Debye length. This agrees well with SFG-results and suggests a considerably increased charge density at the hydrophobic interface at pH = 8. The increased charge density leads to smaller adhesion since the layer is, effectively, less hydrophobic.

DISCUSSION

We measured and controlled the interaction forces between surfaces with surface bonded short-chained amine-terminated PEG and apposing surfaces with self-assembled monolayers by adjusting the chemistry of the apposing surfaces. Figure 6 summarizes the various interactions that were measured, distinguished, and controlled in this study.

The alcohol (OH) terminated SAMs are hydrophilic, and thus fully hydrated, and offer no specific binding sites for the terminal PEG_{27}-NH_2 groups. For this system repulsive steric-polymer and weakly attractive van der Waals forces dominate over any weak and nonspecific hydrogen bondings, and on separating the surfaces only weak or no adhesion is found (Figure 6A).

A carboxylic acid terminated SAM offers specific binding sites for the end-functionalized amine groups of the PEG coils, allowing the formation of specific acid−base bonds. As a result, the PEG coils bridge the apposing surfaces, and on separation the surfaces jump apart at distances D_J around the contour length ($D_J \approx L_C$), where the PEG coils are fully stretched (Figure 6B). Interestingly, the binding between a carboxylic acid and an amine group appears to be a special type of *charge mediated hydrogen bond* that is strong and specific but only if the two involved groups are charged, hence the strong pH dependence. The measured pull-off forces and force−distance profiles between a negatively charged carboxylic acid and a positively charged amine indicate strong hydrogen bonding, which is in the range of $9.5-11 k_BT$ binding energy per bond. The measured magnitude compares well with values expected

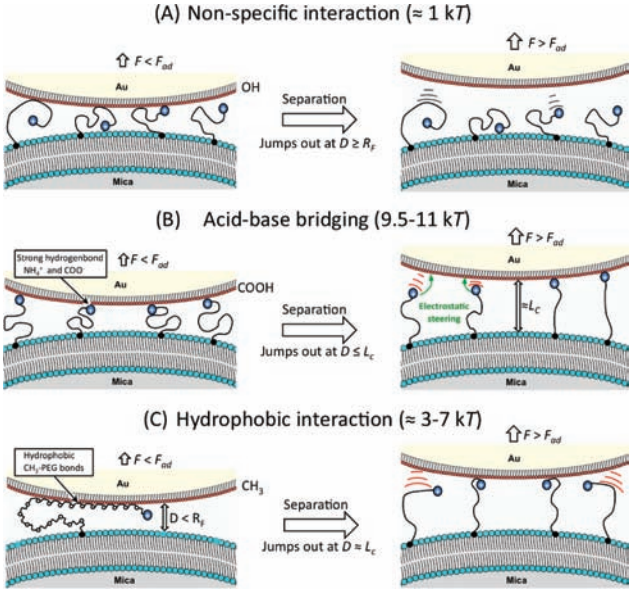

Figure 6. Schematic illustrations of different types of interactions that give rise to the measured forces in the designed system. Typical interaction energies are given per binding for the nonspecific and acid base bond, and per segment for the hydrophobic interaction (cf. text for details). (A) An alcohol (OH) terminated SAM is hydrophilic with no specific binding sites for the end-grafted and end-functionalized PEG_{27}-NH_2 coil. (B) A carboxylic acid terminated SAM offers specific binding sites for the end-functionalized amine of the PEG-coil, allowing the formation of a specific acid−base binding. Even at full extension of the PEG chains, long-range electrostatic interactions trigger steering of the amine head group toward the carboxylic acid terminated SAM. (C) The methyl ($-CH_3$) terminated SAM is strongly hydrophobic and thus attracts the hydrophobic segments of the PEG-coil (cf. text for details).

for strong hydrogen bonds. For instance, the strength of most hydrogen bonds lies within the range of 8−30 kJ/mol or approximately $4-12 k_BT$ per bond.[33]

Scheme 1 shows the proposed bonding mechanisms and resulting hydrogen bonds. The opposite charges of the apposing functional groups lead to a long-range exponentially attractive electrostatic interaction. This long-range interaction leads to an electrostatic "steering" of the tethered amine groups toward the carboxylic acid groups on the SAM surface. Electrostatic steering between oppositely charged functionalities leads to rapid bond formation and considerably higher binding probabilities already at distances around $0.9L_C$ of the PEG tethers (L_C = 10.2 nm), which is greater than the Debye length (λ_D = 4.3 nm), the Flory radius (R_F = 2.5 nm), and the expected critical capture distance[36] of $D_C = 0.75L_C$ for specific bindings with $10 k_BT$ binding energy.[35] As further shown in Scheme 1, the molecular geometry allows the formation of up to two hydrogen bridges, which explains the high binding force exhibited by these systems. The bonding between the acid group and the amine group allows for a sharing of the hydrogen atoms between the oppositely charged functional groups, and consequently the resulting hydrogen bonds are indistinguishable from a hydrogen bonding between two uncharged carboxylic acid and amine functionalities. This specific binding formation is an example for a general mechanism where a nonspecific long-range force (in this case electrostatic) steers two complementary groups rapidly together into their final binding state. Such a *charge-assisted formation of hydrogen bonds*

dx.doi.org/10.1021/ja209653n | J. Am. Chem.Soc. 2012, 134, 1746−1753

Scheme 1. Proposed Mechanism of the *Charge Assisted* Formation of the Hydrogen Binding between Charged Carboxylic Acid and Amine Functionalities[a]

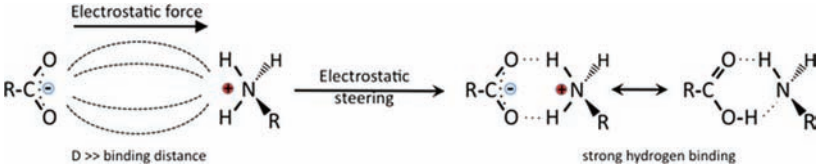

[a]This scheme is an example of a more general mechanism where a nonspecific long-range attraction (in this case electrostatic) steers two complementary groups rapidly into their final and specific binding state.

plays a significant role in many biological processes and assemblies.[2,10,11] Our results allow a direct measurement and quantification of the bond energies and dynamics of individual carboxylic acid amine bonds, which are quite common and thus particularly important in both biological and synthetic systems.

The methyl ($-CH_3$) terminated SAM is strongly hydrophobic and attracts the hydrophobic part of the chain segments of the PEG coil (see Figure 6C). In contact, the surfaces approach to distances $D < R_F$ due to the strong hydrophobic bridging. Upon separation, the force distance profiles also indicate adhesive bridging to be *considerably stronger than the acid–base bridging attraction*. In this case, the PEG coils detach segment-by-segment, with each segment giving rise to a hydrophobic interaction between the two surfaces. Interestingly, a segment-by-segment detachment suggests that PEG chains offer multiple hydrophobic "interaction sites" (i.e., the number of segments). Therefore, the hydrophobic interaction energy per segment can be estimated.[44] From the measured adhesion force profiles, interaction energies of about $6-7k_BT$ per segment at pH = 2.5 and $3k_BT$ at pH 8 per segment were obtained. The magnitude per segment is within the range of typical hydrogen bonds ($4-12k_BT$) and compares well with literature data. For example, hydrophobic interaction energies of −11.3 kJ/mol, or approximately $5k_BT$, were measured for the dimerization of cyclohexane in aqueous solution.[45] In good agreement with previous results, the measured hydrophobic interaction per segment is about 3–7 times stronger compared to van der Waals interactions between hydrocarbons in water ($\approx 1k_BT$). At this point in time, the physical origin and the pH dependence of the hydrophobic interaction are still not fully understood.[40,41]

CONCLUSIONS

We have shown that the interaction forces between differently functionalized SAMs and a surface covered with amine-terminated PEG polymers strongly depend on the charge and hydrophobicity of the SAM surface groups and the solution pH. The binding interaction between carboxylic acid groups and amine functionalities is a *specific and strong hydrogen bonding interaction* only under conditions where the carboxylic acid and amine functionalities are oppositely charged ($pK_{A(COOH)} < pH < pK_{A(amine)}$), whereas the binding is weak and nonspecific at pH values below the pK_A of the carboxylic acid. Our findings also revealed that long-range electrostatic "steering" of acid and base pairs leads to rapid formation of this specific binding even at distances close to full extension of the PEG tethers and at separations larger than the Flory radius of the tethers, the Debye length, and the expected critical binding distance. Due to electrostatic "steering" the charge assisted hydrogen bond formation is driven to form at larger distances, which has important implications for many biological and synthetic processes such as protein folding, enzymatic catalysis, or meso-structuring of soft and nanoscale materials. Compared to the acid–base bonding, the hydrophobic interaction of individual segments leads to a considerably stronger bonding of PEG chains to the hydrophobic SAM. The adhesive bridging observed in these systems arises from a segment-by-segment detachment of individual polymer backbone segments. Finally, our newly developed SFA experiment provides the means for systematic studies of dissimilar interfaces and, in particular, for real-time measurements of the dynamics of molecular recognition and bridging interactions between chemically and molecularly designed apposing model surfaces for biological, medical, and functional material applications.

ASSOCIATED CONTENT

Supporting Information

FECO of force run presented in Figure 5B. This material is available free of charge via the Internet at http://pubs.acs.org.

AUTHOR INFORMATION

Corresponding Author

jacob@engineering.ucsb.edu

ACKNOWLEDGMENTS

M.V. acknowledges financial support through a Marie Curie International Outgoing Fellowship within the seventh European Community Framework Programme (Project No.: IOF-253079). This work was partly supported by the U.S. Department of Energy, Office of Basic Energy Sciences, Division of Materials Sciences and Engineering under Award No. DE-FG02-87ER-45331 (development of SFA instrumentation and other lab equipment).

REFERENCES

(1) Kuhl, T. L.; Leckband, D. E.; Lasic, D. D.; Israelachvili, J. N. *Biophys. J.* **1994**, *66*, 1479.
(2) Nel, A. E.; Maedler, L.; Velegol, D.; Xia, T.; Hoek, E. M. V.; Somasundaran, P.; Klaessig, F.; Castranova, V.; Thompson, M. *Nat. Mater.* **2009**, *8*, 543.
(3) Xia, F.; Jiang, L. *Adv. Mater.* **2008**, *20*, 2842.
(4) Lee, H.; Dellatore, S. M.; Miller, W. M.; Messersmith, P. B. *Science* **2007**, *318*, 426.
(5) Israelachvili, J.; Wong, J.; Kuhl, T. *Abstr. Pap. Am. Chem. Soc.* **1997**, *213*, 8.
(6) Anselme, K. *Biomaterials* **2000**, *21*, 667.
(7) O'Toole, G.; Kaplan, H. B.; Kolter, R. *Annu. Rev. Microbiol.* **2000**, *54*, 49.
(8) Hagleitner, C.; Hierlemann, A.; Lange, D.; Kummer, A.; Kerness, N.; Brand, O.; Baltes, H. *Nature* **2001**, *414*, 293.
(9) Dinner, A. R.; Abkevich, V.; Shakhnovich, E.; Karplus, M. *Proteins: Struct., Funct., Genet.* **1999**, *35*, 34.
(10) Warshel, A. *J. Biol. Chem.* **1998**, *273*, 27035.

(11) Wade, R. C.; Gabdoulline, R. R.; Ludemann, S. K.; Lounnas, V. *Proc. Natl. Acad. Sci. U.S.A.* **1998**, *95*, 5942.
(12) Stupp, S. I.; LeBonheur, V.; Walker, K.; Li, L. S.; Huggins, K. E.; Keser, M.; Amstutz, A. *Science* **1997**, *276*, 384.
(13) Yang, P. D.; Zhao, D. Y.; Margolese, D. I.; Chmelka, B. F.; Stucky, G. D. *Chem. Mater.* **1999**, *11*, 2813.
(14) Kitagawa, S.; Kitaura, R.; Noro, S. *Angew. Chem., Int. Ed.* **2004**, *43*, 2334.
(15) Israelachvili, J.; Pashley, R. *Nature* **1982**, *300*, 341.
(16) Leckband, D.; Israelachvili, J. *Q. Rev. Biophys.* **2001**, *34*, 105.
(17) Levinthal, C. *J. Chim. Phys. Phys.-Chim. Biol.* **1968**, *65*, 44.
(18) Na, K.; Jo, C.; Kim, J.; Cho, K.; Jung, J.; Seo, Y.; Messinger, R. J.; Chmelka, B. F.; Ryoo, R. *Science* **2011**, *333*, 328.
(19) Min, Y.; Akbulut, M.; Kristiansen, K.; Golan, Y.; Israelachvili, J. *Nat. Mater.* **2008**, *7*, 527.
(20) Velikov, K. P.; Velev, O. D. *Curr. Opin. Colloid Interface Sci.* **2011**, *16*, 81.
(21) Velev, O. D.; Gupta, S. *Adv. Mater.* **2009**, *21*, 1897.
(22) Bain, C. D.; Troughton, E. B.; Tao, Y. T.; Evall, J.; Whitesides, G. M.; Nuzzo, R. G. *J. Am. Chem. Soc.* **1989**, *111*, 321.
(23) Love, J. C.; Estroff, L. A.; Kriebel, J. K.; Nuzzo, R. G.; Whitesides, G. M. *Chem. Rev.* **2005**, *105*, 1103.
(24) Hegner, M.; Wagner, P.; Semenza, G. *Surf. Sci.* **1993**, *291*, 39.
(25) Jeppesen, C.; Wong, J. Y.; Kuhl, T. L.; Israelachvili, J. N.; Mullah, N.; Zalipsky, S.; Marques, C. M. *Science* **2001**, *293*, 465.
(26) Wong, J. Y.; Kuhl, T. L.; Israelachvili, J. N.; Mullah, N.; Zalipsky, S. *Science* **1997**, *275*, 820.
(27) Israelachvili, J.; Min, Y.; Akbulut, M.; Alig, A.; Carver, G.; Greene, W.; Kristiansen, K.; Meyer, E.; Pesika, N.; Rosenberg, K.; Zeng, H. *Rep. Prog. Phys.* **2010**, 73.
(28) Israelachvili, J. N.; McGuiggan, P. M. *Science* **1988**, *241*, 795.
(29) Valtiner, M.; Kristiansen, K.; Greene, G. W.; Israelachvili, J. N. *Adv. Mater.* **2011**, *23*, 2294.
(30) Chai, L.; Klein, J. *Langmuir* **2007**, *23*, 7777.
(31) Chai, L.; Klein, J. *Langmuir* **2009**, *25*, 11533.
(32) Hogg, R.; Healy, T. W.; Fuerstenau, D. W. *Trans. Faraday Soc.* **1966**, *62*, 1638.
(33) Israelachvili, J. N. *Intermolecular and Surface Forces*, 3rd ed.; Academic Press: 2011.
(34) Alexander, S. *J. Phys. (Paris)* **1977**, *38*, 983.
(35) The binding energy of individual carboxylic acid amine bonds E_{AB} was calculated using: $F(D_J) = -2\cdot\pi\cdot R\cdot\sigma\cdot E_{AB}$ (Derjaguin approximation; see also refs 33, 26). An adhesion force of F/R = 6−7 mN/m, and thus an adhesion energy of 0.95−1.1 mJ/m^2, or approximately 9.5−11kT, per acid−base bond was calculated. Fitting of the measured maximum-bridging force to the analytical equation for tethered ligand−receptor bonds from ref 36. (spring model; using a tether spring constant of 3 mN/m and the experimental parameters for σ) gives a comparable value of 10kT per bond for the acid−base bond energy. The critical bond capture distance D_C was calculated to be 7.5 nm.
(36) Moore, N. W.; Kuhl, T. L. *Biophys. J.* **2006**, *91*, 1675.
(37) Markley, J. L.; Westler, W. M. *Biochemistry* **1996**, *35*, 11092.
(38) Kauzmann, W. *Adv. Protein Chem.* **1959**, *14*, 1.
(39) Godawat, R.; Jamadagni, S. N.; Garde, S. *Proc. Natl. Acad. Sci. U.S.A.* **2009**, *106*, 15119.
(40) Hammer, M. U.; Anderson, T. H.; Chaimovich, A.; Shell, M. S.; Israelachvili. *Faraday Disc.* **2010**, *146*, 299.
(41) Meyer, E. E.; Rosenberg, K. J.; Israelachvili, J. *Proc. Natl. Acad. Sci. U.S.A.* **2006**, *103*, 15739.
(42) Scatena, L. F.; Brown, M. G.; Richmond, G. L. *Science* **2001**, *292*, 908.
(43) Scatena, L. F.; Richmond, G. L. *J. Phys. Chem. B* **2001**, *105*, 11240.
(44) A segment-by-segment detachment of the hydrophobic backbone segments is physically similar to plucking out a lipid from a lipid-bilayer.[26] Thus, the hydrophobic interaction energy of individual segments E_S can be calculated from the regime of constant force in the separation profiles (see Figure 5B) according to $F = -1.5\cdot\pi\cdot R\cdot n_B\cdot\sigma\cdot E_S$, where $n_B = f_B\cdot n$ is the number of individual segments bound to the hydrophobic surface per chain, and f_B is the fraction of segments bound (see ref 26). The fraction of bound chain segments is about f_B = 0.8−1, which gives hydrophobic interaction energies within the range of 6−7kT per segment.
(45) Tucker, E. E.; Lane, E. H.; Christian, S. D. *J. Solution Chem.* **1981**, *10*, 1.